TRACE ELEMENT AND ISOTOPIC CONSTRAINTS ON THE FORMATION AND CRYSTALLIZATION OF A TYPE B1 CAI FROM ALLENDE.

A. K. Kennedy[1], J. R. Beckett and I.D. Hutcheon[1]. Division of Geological & Planetary Sciences, Caltech, Pasadena, CA 91125. [1]Also inmates of The Lunatic Asylum.

Introduction. The chemical and isotopic compositions of minerals and the partitioning of trace elements between phases constrain the formation and evolution of Ca-Al-rich inclusions (CAI) [1,2]. Some of these CAI were at least partially melted [3] and may provide information on events before, during and after the most recent crystallization period. We measured Ba and REE abundances and Mg isotopes of phases in USNM 3655A, an Allende Type B1 inclusion [4,5] using the PANURGE ion microprobe with techniques and standards of [6,7].

3655A has a melilite(Mel)-rich mantle (<Ak5-Ak64) surrounding a core composed of clinopyroxene (Cpx), anorthite (An), spinel (Sp) and Mel. Mantle Mel contains minor included perovskite (Pv), Cpx, An and Sp. Some Cpx in the core of the inclusion have possibly relict cores [5] exhibiting patchy variations in TiO_2 (3-13%). Sp, which is concentrated in the core of the inclusion, occurs as large euhedral crystals and as palisades [4]. 3655A has a flat REE pattern at ~20× chondritic (ch) abundances [8].

Trace Element Results. Mantle Mel has a LREE-enriched pattern (La, 4-24×ch; Er, 1-16×ch) and a positive Eu anomaly (Eu, 18-38×ch). Fig. 1 shows the concentrations of a divalent (Eu) and trivalent (La) cation plotted against X_{Ak}. A concave downward pattern, characteristic of all trivalent REE in 3655A, is also observed in Type B1's 3529Z and Egg 6 [11]. It is quite different from the monotonically decreasing pattern observed in USNM 5241 [9] and synthetic Mel [6]. The behavior of Ba^{2+} is similar to that of Eu. Dramatic changes in trace element abundances are observed within 30μm of inclusions. Relative to Mel of equal X_{Ak}, Mel adjacent to Sp is enriched in the REE (e.g., La up to 47×ch), while Mel adjacent to Pv is depleted. Cpx is depleted in the LREE (e.g., La, 6-15×ch) and Eu (3-6×ch) relative to the HREE (e.g., Er, 34-68×ch). Trace element zoning patterns for Cpx are shown in Fig. 2. Trivalent REE increase smoothly and Ti decreases as crystallization proceeds. There are no significant trace element differences between the patchy Cpx cores and Cpx overgrowths. Pv is REE-enriched (La, 100-550×ch) and has a relatively flat pattern for the light to middle REE, a negative Eu anomaly and lower HREE abundances (e.g., Yb < 50-100×ch).

Isotopic Results. Mg isotopic compositions are given as δ^{26}Mg relative to 0.13955 and as mean F_{Mg} calculated from the measured $^{25}Mg/^{24}Mg$ ratio relative to terrestrial standards. δ^{26}Mg and $^{27}Al/^{24}Mg$ are positively correlated and An has large δ^{26}Mg values (up to 102±5‰). The calculated slope of 3.9×10^{-5} for $^{26}Mg^{*}/^{27}Al$ is similar to the values for other Allende Type B1 inclusions [2]. Sp and Cpx have isotopically heavy Mg with variable F_{Mg}. The patchy Cpx cores (F_{Mg}=3.9±1.5‰/amu), surrounding Cpx overgrowths (F_{Mg}=3.4±1.5‰/amu) and Sp from the inclusion core (F_{Mg}=4.7±1.5‰/amu) have similar isotopic compositions. Sp from one palisade within the Mel-rich mantle is more enriched in heavy Mg (F_{Mg}=8.3±1.5‰/amu) than the bulk of the inclusion.

Discussion. Mel/liquid distribution coefficients [D(Mel/L)] for divalent cations are roughly constant in CAI melts [6] as shown by concentration-X_{Ak} plots (e.g., Fig. 1). A D_{Eu} of ~0.5 has been calculated from the zoning profile of 3655A and this value is close to the experimentally determined D(Mel/L) = 0.6 for Sr [10]. The sharp drop in C_{Eu} at ~Ak40 is most likely due to onset of An crystallization in the core. The concave downward pattern of trivalent REE concentrations as a function of Ak (Fig. 1), which occurs in other Type B1 CAI [11], may be due to trace element enriched boundary layers at the surface of growing Mel crystals and/or subsolidus reequilibration of zoned Mel. If the observed zoning pattern reflects crystallization, then D(Mel/L)

is < ~0.5 for Mel ≤ Ak10; a much lower D than values extrapolated from [6]. In addition, D(Mel/L) for high Ak Mel must be substantially higher than experimental values. The sharp contrast in zoning profiles for trivalent REE between synthetic Mel [6] and mantle Mel from most Type B1's has broad implications for the crystallization histories of these inclusions. It is notable that zoning patterns of divalent cations in mantle Mel are consistent with data of [6]. Since divalent cations diffuse much more rapidly in silicate melts than trivalent cations [12] it is possible that Mel growth rates were slow enough to allow homogenization of the divalent cations in the melt but sufficiently fast to cause enrichment of the trivalent cations in the boundary layer at the Mel/L interface.

The lack of isotopic or trace element differences between the patchy cores and the normal overgrowths in Cpx suggests that the odd patchy material is not exotic. In contrast, there is isotopic disequilibrium between Sp from palisades and the bulk of the inclusion, suggesting that some Sp predate the melting event and that the precursor of 3655A was isotopically heterogeneous. Trace element enrichment in Mel and Cpx near Sp may result from rapid crystallization of both Cpx and Mel (± Sp) trapping of melt that is enriched in incompatible elements near the Sp. Trace element depleted Mel adjacent to Pv may have grown from melt depleted by Pv or reflect subsolidus reequilibration. Pv may be relict as it is not stable during early crystallization in Type B bulk compositions [3]. Our data suggest that crystal/liquid partitioning of trace elements during crystallization of most Type B1's was strongly influenced by kinetic effects. (#697)

References. [1] Kennedy A.K. et al. (1989) LPS XX, 514. [2] Huneke J.C. et al. (1983) GCA 47, 1635. [3] Stolper E.M. and Paque J.M. (1986) GCA 50, 1785. [4] Wark D.A. and Lovering J.F. (1982) GCA 46, 2595. [5] Paque J.M. (1990) this volume. [6] Beckett J.R. (1990) GCA, submitted. [7] Hutcheon I.D. et al. (1987) GCA 51, 3175. [8] Mason B. and Taylor S.R. (1982) SCES 25, 1. [9] MacPherson G.J. et al. (1989) GCA 53, 2413. [10] Woolum D.S. et al. (1988) LPS XIX, 1294. [11] Kennedy A.K. et al. (1988) Meteoritics 23, 279. [12] Hofmann A.W. (1980) p. 385 in Hargraves R.B. Physics of Magmatic Process.

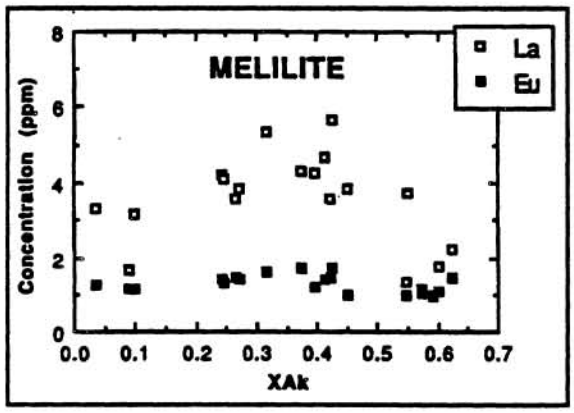

Fig. 1. Concentrations of La and Eu in mantle Mel as a function of X_{Ak}. Analyses within 30μm of inclusions are excluded.

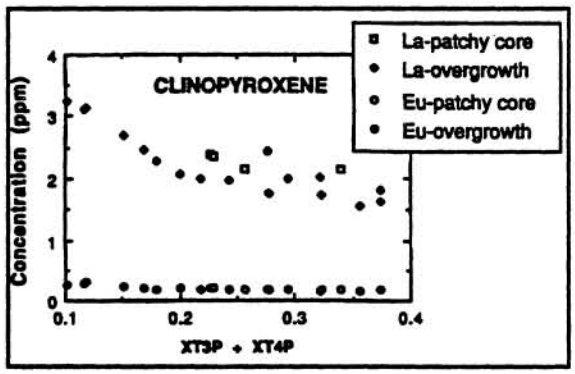

Fig. 2. Concentrations of La and Eu in Cpx with patchy zoned cores as a function of the sum of the mole fractions of $CaTi^{3+}AlSiO_6$ (T_3P) and $CaTi^{4+}Al_2O_6$ (T_4P). Crystallization proceeds from Ti-rich to Ti-poor. The Ca-Tschermak's (CaTs)/Diopside (Di) ratio increases with decreasing Ti. Analyses within 30μm of inclusions are excluded.